

Role of PufX in Photochemical Charge Separation in the RC-LH1 Complex from *Rhodobacter sphaeroides*: An Ultrafast Mid-IR Pump–Probe Investigation

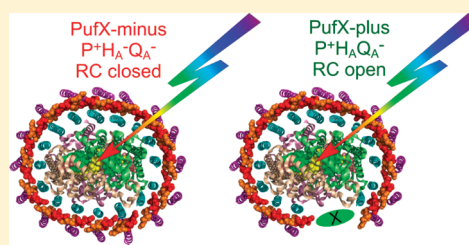
Andreas D. Stahl,[†] Lucy I. Crouch,[‡] Michael R. Jones,[‡] Ivo van Stokkum,[†] Rienk van Grondelle,[†] and Marie Louise Groot^{*,†}

[†]Department of Physics and Astronomy, Faculty of Sciences, VU University Amsterdam, Amsterdam, The Netherlands

[‡]School of Biochemistry, Medical Sciences Building, University of Bristol, University Walk, Bristol BS8 1TD, United Kingdom

Supporting Information

ABSTRACT: Photochemical charge separation in isolated reaction center-light harvesting 1 (RC-LH1) complexes from *Rhodobacter sphaeroides* was examined using time-resolved mid-infrared pump–probe spectroscopy. Absorption difference spectra were recorded between 1760 and 1610 cm^{-1} with subpicosecond time resolution to characterize excited-state and radical pair dynamics in these complexes, via the induced absorption changes in the keto carbonyl modes of the bacteriochlorophylls and bacteriopheophytins. Experiments on RC-LH1 complexes with and without the polypeptide PufX show that its presence is required to achieve generation of the radical pair $\text{P}^+\text{Q}_\text{A}^-$ under mildly reducing conditions. In the presence of PufX, the final radical pair formed over a ~ 3 ns period was $\text{P}^+\text{Q}_\text{A}^-$, but in its absence the corresponding radical pair was $\text{P}^+\text{H}_\text{A}^-$, implying that Q_A was either absent in these PufX-deficient complexes or was prerduced. However, $\text{P}^+\text{Q}_\text{A}^-$ could be generated in PufX-deficient complexes following addition of the oxidant DMSO, showing that Q_A was present in these complexes and allowing the conclusion that under mildly reducing conditions charge separation was blocked after $\text{P}^+\text{H}_\text{A}^-$ due to the presence of an electron on Q_A . The data provide strong support for the hypothesis that one of the functions of PufX is to regulate the stability of Q_B^- , ensuring the oxidation of Q_A^- in the presence of a reduced quinone pool and so preserving efficient photochemical charge separation under anaerobic conditions.



INTRODUCTION

Much of our understanding of the molecular mechanism of photosynthetic energy transduction has come from studies of the structure and spectroscopic properties of the purple bacterial reaction center (RC), and in particular the complex from the species *Rhodobacter (Rba.) sphaeroides*.^{1–9} The bulk of this work has involved analysis of detergent-solubilized and purified *Rba. sphaeroides* RCs, with less emphasis on the “inner workings” of the RC when part of more intact systems. A combination of structural biology, ultrafast spectroscopy and steady-state spectroscopy has revealed that the RC uses the energy of absorbed photons to power a picosecond-time scale, three-step, membrane-spanning charge separation involving a dimer of bacteriochlorophyll (BChl) as the primary electron donor (denoted P), a monomeric BChl (B_A), a bacteriopheophytin (H_A), and a tightly bound ubiquinone-10 (Q_A) as sequential electron acceptors (Figure 1b).^{1–9} The first singlet excited state of the P dimer (denoted P^*) decays to form the $\text{P}^+\text{B}_\text{A}^-$ radical pair with a lifetime of 3–5 ps, with a second step of electron transfer to form $\text{P}^+\text{H}_\text{A}^-$ in less than 1 ps. The $\text{P}^+\text{H}_\text{A}^-$ radical pair has a lifetime of ~ 200 ps, decaying principally to form $\text{P}^+\text{Q}_\text{A}^-$ (Figure 1b). Q_A passes two electrons, sequentially, to a second dissociable ubiquinone at the Q_B site, generating, with the uptake of two protons, dihydroquinone (ubiquinol).^{10,11} In the intact *Rba. sphaeroides*

cell, the photo-oxidized P dimer is reduced by a water-soluble cytochrome (cyt) c_2 ,¹² and the products of RC turnover, ubiquinol and oxidized cyt c_2 , act as substrates for the protonmotive cyt bc_1 complex.

A detailed picture of the mechanism of the membrane-spanning charge separation internal to the RC has been built up through the extensive application of ultrafast visible/near-infrared (IR) transient absorbance spectroscopy (reviewed in refs 4–7) and, to a lesser extent, ultrafast mid-IR transient absorbance spectroscopy.^{13–21} However, the RC is only part of the sunlight transduction system in photosynthetic organisms. In all known purple photosynthetic bacteria, the RC is associated with a light harvesting 1 (LH1) pigment–protein, forming the so-called RC-LH1 complex.^{22–26} The precise composition of this complex varies from species to species, but in general terms the LH1 forms a hollow cylinder of membrane-spanning α -helices and associated BChl and carotenoid cofactors that surrounds a central RC.^{22–26} In some species, this cylinder appears to be complete, with ~ 32 LH1 BChls forming a ring that feeds the RC with excited state energy, while in other species, including *Rba. sphaeroides*,

Received: July 14, 2011

Revised: December 1, 2011

Published: December 06, 2011

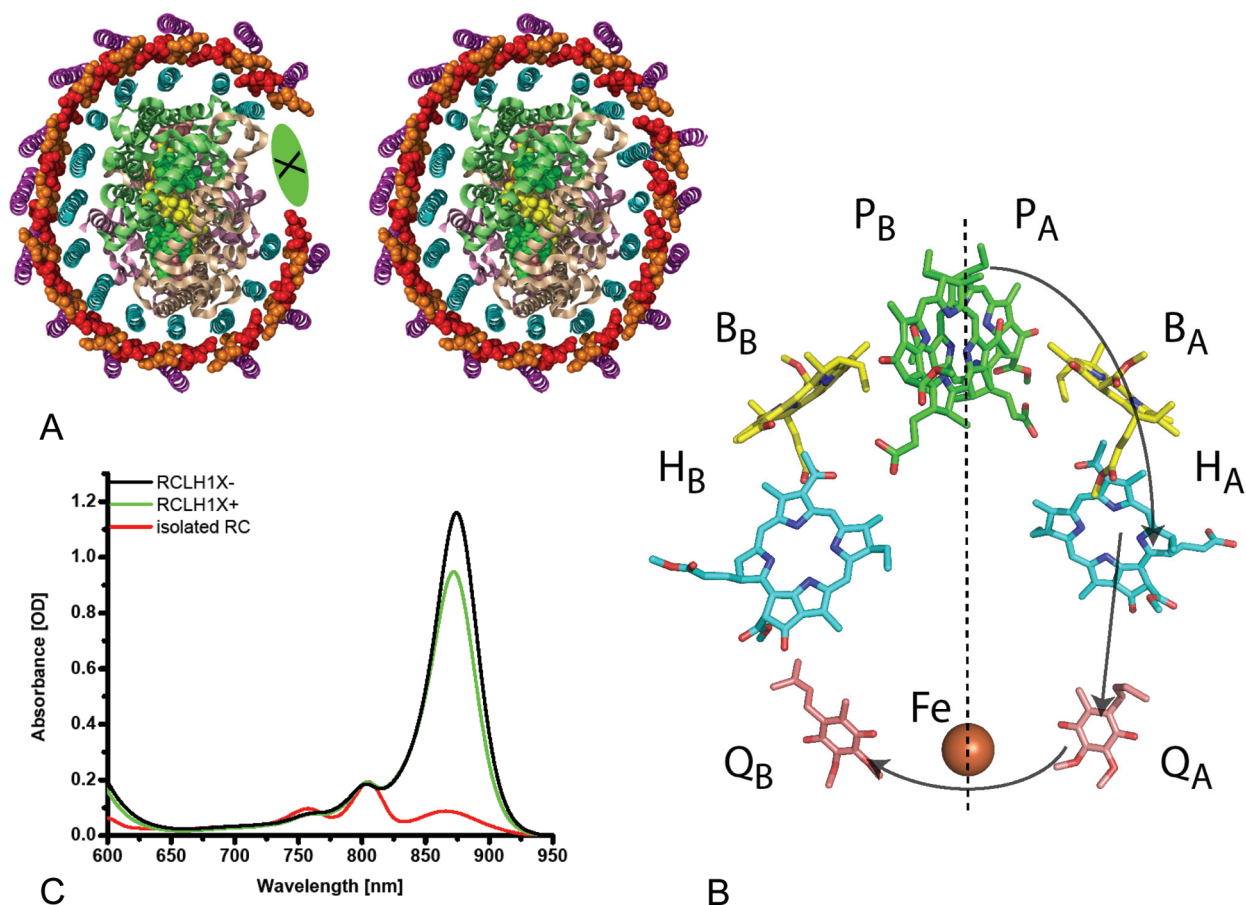


Figure 1. (A) Periplasmic views of schematics of the PufX-containing (left) and PufX-deficient (right) RC-LH1 complexes used in this work, based on modifications of a 4.8 Å X-ray crystal structure of the RC-LH1 complex from *Rhodospseudomonas palustris*.²⁵ The central RC (green, beige and pink ribbons) is surrounded by an LH1 antenna pigment–protein comprising an inner ring of α -polypeptides (cyan ribbons) and an outer ring of β -polypeptides (magenta ribbons), each of which has a single membrane-spanning α -helix. Between these concentric LH1 protein cylinders is a ring of BChls (shown as spheres alternating red/orange) that absorb at 875 nm. In native *Rba. sphaeroides* PufX occupies the approximate position shown by the green ellipse and interrupts the continuity of the LH1 ring (left). In the absence of PufX, this ring is complete due to the presence of additional LH1 pigment–protein (right). (B) Arrangement of the pigments in the reaction center of *Rba. sphaeroides*. The BChl, BPhe and ubiquinone cofactors form two membrane-spanning branches, denoted A and B. The dotted line shows the axis of 2-fold symmetry, arrows indicate the pathway of electron transfer. The picture was created using the PDB entry 2BOZ.⁹⁰ (C) Absorption spectra of isolated RC (red), RC-LH1-X+ (green) and RC-LH1-X- (black) complexes.

the cylinder is incomplete, with 24–30 LH1 BChls forming an arc around the central RC (Figure 1A, left) (see refs 27–29 for reviews). In *Rhodobacter* species, the RC-LH1 complex is also known to contain a polypeptide termed PufX that has a single membrane-spanning α -helix and has a strong influence on the structure of the RC-LH1 complex (see ref 30 for a detailed review). In *Rba. sphaeroides*, the RC-LH1 complex assembles in a dimeric form in which two RCs are surrounded and connected by an S-shaped LH1 antenna^{31–37} and a monomeric form is also observed where the RC is surrounded by an open C-shaped antenna³¹ (Figure 1A). When PufX is removed from *Rba. sphaeroides* through a gene deletion, the dimeric RC-LH1 complex is no longer assembled, and the monomeric complex has a larger, intact ring of LH1 pigment protein surrounding the RC (Figure 1A).^{37,38} Removal of PufX also leads to a loss of capacity for photosynthetic growth, for reasons that are not fully understood (see ref 30 for a review of the original literature).

In the present work, ultrafast mid-IR spectroscopy was used to probe the characteristics of charge separation in isolated PufX-containing and PufX-deficient monomeric RC-LH1 complexes, comparing the difference spectra obtained with

those from isolated RCs. To our knowledge, this is the first application of ultrafast spectroscopy to *Rba. sphaeroides* RC-LH1 complexes that have been removed from the photosynthetic membrane. Although it is well-known that interrogation of charge separation by ultrafast spectroscopy is complicated by the presence of an excess of antenna pigments, it has recently been shown that states functionally equivalent to the $P^+H_A^-$ and $P^+Q_A^-$ radical pairs described above can be resolved in Photosystem II core complexes^{39,40} and in intact Photosystem I complexes⁴¹ through the application of ultrafast mid-IR spectroscopy. In addition to examining whether the LH1 pigment–protein environment modulates the characteristics of charge separation in the RC, we provide evidence for a proposed mechanistic basis of the loss of photosynthetic competence that accompanies removal of PufX from the *Rba. sphaeroides* RC-LH1 complex.

MATERIALS AND METHODS

Biological Material. All *Rba. sphaeroides* strains were grown under dark/semiaerobic conditions using M22+ medium⁴²

supplemented with neomycin and tetracycline.⁴³ Starter cultures comprising 10 mL of M22+ medium in a 30 mL universal bottle were inoculated with cells taken from a glycerol stock and grown for 24 h at 34 °C and 180 rpm in a darkened orbital incubator. Each of these were then used to inoculate 70 mL of M22+ medium in a 100 mL conical flask, and after further growth for 24 h, this intermediate culture was used to inoculate 1.5 L of M22+ medium in a 2 L conical flask. These large volume cultures were incubated for 36 h, harvested by centrifugation, and intracytoplasmic membranes were prepared by cell lysis in a French pressure cell followed by ultracentrifugation, as described previously.^{43,44}

Rba. sphaeroides RCs were prepared from an antenna-deficient strain⁴⁴ as described in detail elsewhere.⁴⁵ Purified RCs were stored as a concentrated solution in 20 mM Tris/HCl (pH 8.0)/0.1% lauryldimethylamine oxide (LDAO), and kept at −80 °C until used.

Monomeric *Rba. sphaeroides* RC-LH1-X+ complexes were prepared from a strain lacking the LH2 antenna complex, and RC-LH1-X− complexes were prepared from a strain lacking LH2 and the PufX protein.⁴⁶ Both types of complex were isolated from intracytoplasmic membranes using 4% β -dodecyl maltoside (β -DDM),^{35,47} purified by ultracentrifugation on a five-step 20–25% (w/v) sucrose density gradient,⁴⁷ and stored as a concentrated solution in 20 mM HEPES (pH 8.0)/0.04% DDM at −80 °C until used.

Sample Preparation. For vis/mid-IR experiments, the sample was concentrated to an absorbance of 0.2 at 800 nm for a 20 μ m optical path length. Purified RCs were suspended in 20 mM Tris-buffer in D₂O (pD 7.6) containing 0.1% LDAO, 25 μ M phenazine methosulfate (PMS) and 5 mM sodium ascorbate. In the case of RC-LH1 complexes, two different buffers were used. The first consisted of 20 mM HEPES buffer in D₂O (pD 7.6) with 0.04% β -DDM, 25 μ M PMS, and 5 mM sodium ascorbate. The other contained 20 mM HEPES buffer in D₂O (pD 7.6) with 0.04% β -DDM and 20 mM dimethylsulfoxide (DMSO). Absorption spectra were recorded with a Lambda 40 spectrophotometer (Perkin-Elmer).

Pump–probe spectroscopy. The experimental setup consisted of an integrated Ti:sapphire oscillator-regenerative amplifier laser system (Hurricane, SpectraPhysics) operating at 1 kHz and 800 nm, producing 85 fs pulses of 0.8 mJ.⁴⁸ A portion of the 800 nm light was used as the pump pulse with a pulse energy of 100 nJ. The excitation pulses were focused on the sample with a 20 cm lens. A second part of the 800 nm light was used to pump an optical parametric generator and amplifier with a difference frequency generator (TOPAS, Light Conversion) to produce the mid-IR probe pulses, which were focused on the sample with a 6 cm lens. The probe and pump pulses were spatially overlapped in the sample, and after passing the sample, the probe pulses were dispersed in a spectrograph (resolution 3 cm^{−1}), imaged on a 32-element MCT detector and fed into 32 home-built integrate and hold devices that were read out every shot with a National Instruments acquisition card. The spectral width of the probe pulse was sufficient to probe a 190 cm^{−1} spectral window with 6 cm^{−1} sampling. Typically, a few channels at the edge of the window were omitted from the analysis because of poor signal-to-noise ratio due to low probe light intensity. To ensure a fresh spot for each laser shot, the sample was moved by a home-built Lissajous scanner. The polarization of the excitation pulse was set to the magic angle (54.7°) with respect to the IR probe pulses, and a phase-locked chopper operating at 500 Hz was used to ensure that the sample was excited only on every other shot such

that the change in transmission could be measured. The instrument response function was about 120 fs, and all measurements were performed at room temperature.

Data Analysis. A set of 100 scans for all 32 channels was averaged and 69 time points per scan were taken. Each time point was the average value of 500 laser pulses. All the collected data points were subjected to global analysis using a sequential model with increasing lifetimes.⁴⁹ The spectra are represented by a smooth line (spline function) connecting all data points.

RESULTS

Absorbance Spectra and Experimental Conditions. This study compared charge separation in isolated *Rba. sphaeroides* RCs with that in isolated monomeric PufX-containing RC-LH1 complexes (denoted RC-LH1-X+) and isolated monomeric PufX-deficient RC-LH1 complexes (denoted RC-LH1-X−). The complexes were isolated from intracytoplasmic membranes prepared from cells grown under semiaerobic conditions in the dark, as described in the Materials and Methods section.

Figure 1c shows the Q_y absorbance spectra of the three complexes, normalized to the same absorbance at ~802 nm. In this spectral region, the LH1 antenna has a single band with a maximum at ~870 nm, whereas the RC has three bands with maxima at 756 nm arising from the bacteriopheophytins, 802 nm arising mainly from the monomeric BChls, and 867 nm arising from the primary donor BChl pair. In the RC-LH1 complexes, the absorbance of LH1 at 870 nm dominates the spectrum, the 802 and 756 nm bands of the RC appear as minor components, and the 867 nm band of the RC is obscured. In PufX-deficient RC-LH1 complexes, the ratio of LH1 absorbance to RC absorbance was increased due to the presence of additional BChls, in line with expectations (see above).

In this near-infrared spectral region between 650 and 950 nm absorbance changes occurring on an ultrafast time scale are dominated by the LH1 component (see Figure S1 of the Supporting Information), and the P⁺H_L[−] and P⁺Q_A[−] radical pairs do not have readily distinguished absorbance difference spectra. Therefore we examined a section of the mid-IR region, where it is known from Fourier transform IR (FTIR) difference spectroscopy^{50–56} and ultrafast absorbance difference spectroscopy^{18,39–41} that the H_A/H_A[−] and Q_A/Q_A[−] transitions give rise to distinctive signatures of positive and negative bands. To probe function, RC and RC-LH1 complexes were excited at 800 nm, and the induced absorption changes were probed in the mid-IR spectral region between 1730/1760 and 1610 cm^{−1} from −15 ps to 3 ns. The particular focus was to characterize the difference spectrum of the final radical pair achieved in the different complexes during the 3 ns measuring period. The collected time traces were subjected to a global analysis using a sequential scheme with increasing lifetimes in order to visualize the dynamics occurring in the system after excitation. In the limited number of previous studies of excitation trapping in *Rba. sphaeroides* RC-LH1 complexes,^{57–61} sodium ascorbate and/or PMS was added to prevent photoaccumulation of RCs in the P⁺ state (see Discussion). Accordingly, initial measurements were made in a buffer supplemented with 25 μ M PMS and 5 mM sodium ascorbate to provide comparable conditions (see Materials and Methods).

Ultrafast Mid-IR Spectroscopy of RCs. In the case of the RC, three components were necessary to obtain a satisfactory fit of the experimental data, with lifetimes of 4.1 ps, 250 ps, and >3 ns (infinite). The evolution associated difference spectra (EADS) of

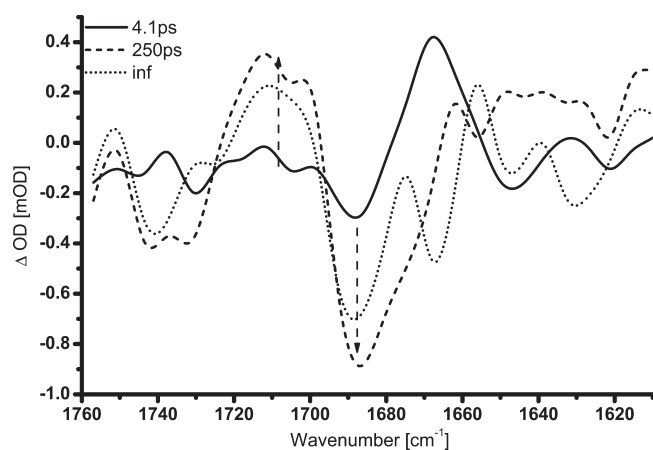


Figure 2. EADS obtained from the RC of *Rba. sphaeroides* after 800 nm excitation, using a global analysis with increasing lifetimes of 4.1 ps (solid to dashed spectrum), 250 ps (dashed to dotted spectrum), and an infinite (long-lived) component (dotted line).

these components are shown in Figure 2. The first EADS (Figure 2, solid) was typical for a BChl excited-state difference spectrum in which the keto carbonyl mode, at $\sim 1685\text{ cm}^{-1}$, downshifts to 1668 cm^{-1} in the excited state, and was therefore consistent with P^* (see ref 18 for a detailed account).

This initial component decayed with a lifetime of 4.1 ps into a second component, the EADS of which (Figure 2, dashed line) displayed positive bands at 1702 cm^{-1} and 1712 cm^{-1} , together with a negative band centered at 1687 cm^{-1} . The latter can be assigned to an unresolved mixture of the 9-keto modes of P_A and P_B in the ground state, which have been resolved by FTIR at 1683 cm^{-1} and 1692 cm^{-1} , whereas the 1702 cm^{-1} and 1712 cm^{-1} bands are due to the keto carbonyls of P_A and P_B in the cation state.^{52,62,63} As discussed in detail previously,¹⁸ the line shape of this second EADS was consistent with the radical pair $P^+H_A^-$. The bacteriopheophytin contribution in this EADS was the weak negative shoulder at 1675 cm^{-1} , which has been ascribed to the 9-keto carbonyl of H_A in the neutral state, being hydrogen bonded to Glu L104.⁶⁴ Upon charge separation, this mode undergoes a very strong downshift to 1591 cm^{-1} accounting for the strongly positive signal appearing at the lower edge of the spectral window. The 1656 cm^{-1} local minimum in the $P^+H_A^-$ spectrum has been assigned to an amide response, resulting from either an upshift to 1662 cm^{-1} in response to the formation of $P^+H_A^-$,^{16,17,53,54} or, in an alternative interpretation, from a downshift to 1648 cm^{-1} .^{52,64}

The second EADS decayed with a lifetime of 250 ps into the final EADS (Figure 2, dotted line), which showed a number of distinctive changes associated with the transition of $P^+H_A^-$ into $P^+Q_A^-$, including the recovery of the bleaching at 1675 cm^{-1} and the appearance of a $1667(-)/1656(+)\text{ cm}^{-1}$ bandshift, ascribed to a protein amide I response to the charge on Q_A^- .¹⁶ The $1647(-)/1640(+)$ signal has been attributed to the response of a protein backbone $C=O$ that is connected to Q_A^- via an H-bond that is perturbed upon reduction of Q_A^- .^{52,53,65}

The features of these three EADS recorded for RCs in the presence of sodium ascorbate and PMS were fully consistent with previous data on mid-IR spectroscopy of *Rba. sphaeroides* RCs in the absence of reductant.^{13,14,16–18} Although EADS reflect the spectral evolution of the system rather than representing pure states, the fact that each step of charge separation in the RC is

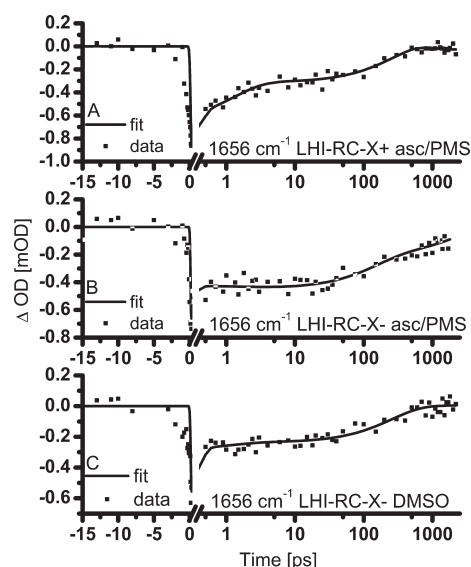


Figure 3. Representative time traces (scattered points) recorded at 1656 cm^{-1} for LHI-RC-X- and LHI-RC-X+ complexes in ascorbate/PMS buffer and LHI-RC-X- complexes in DMSO, and the fit through the data (solid line). The time axis is linear before $t = 0$ and logarithmic after.

slower than the last means that the three EADS can be attributed to P^* (4.1 ps), $P^+H_A^-$ (250 ps), and $P^+Q_A^-$ (infinite). Of particular relevance to the present report are the spectral signatures of Q_A/Q_A^- and H_A/H_A^- , discussed above, and in more detail in ref 18. The infrared difference spectrum of Q_A/Q_A^- shows the sequence $1667(-)/1656(+)/1647(-)/1640(+)$, whereas the infrared difference spectrum of H_A/H_A^- shows the sequence $1662(+)/1656(-)/1648(+)$. Particularly marked is the inversion between $1662(+)/1656(-)$ for H_A/H_A^- and $1667(-)/1656(+)$ for Q_A/Q_A^- .

Ultrafast Mid-IR spectroscopy of RC-LH1-X+ Complexes.

Figure 3A shows a representative time trace at a single wavenumber for the RC-LH1-X+ complex in ascorbate/PMS buffer, showing the quality of the fit from the global analysis. Equivalent traces for RC-LH1-X- complexes in ascorbate/PMS and RC-LH1-X- complexes in an alternative buffer are also shown in Figure 3B,C (see below).

In the case of the monomeric RC-LH1-X+ complex in PMS/ascorbate buffer, a set of three components was necessary to fit the spectral evolution, with lifetimes of 1.3 ps, 130 ps, and $>3\text{ ns}$ (infinite). The initial EADS was dominated by a negative band at 1648 cm^{-1} and a positive band at 1632 cm^{-1} (Figure 4A, solid). In addition, the spectrum displayed a small positive band at 1680 cm^{-1} , a negative band at $\sim 1670\text{ cm}^{-1}$ and a positive band at 1617 cm^{-1} . This initial component decayed in 1.3 ps into a second component (Figure 4A, dashed) with an EADS that showed some changes in line shape, most notably a switch from positive to negative at 1680 cm^{-1} and an approximately 40% decrease in amplitude of the positive band at $\sim 1632\text{ cm}^{-1}$, together with a small ($\sim 2\text{ cm}^{-1}$) upshift). By contrast, the bleach at 1648 cm^{-1} only slightly decreased and somewhat upshifted ($\sim 1\text{ cm}^{-1}$). The EADS of the infinite component (Figure 4A, dotted), formed in 130 ps, showed a further development of the positive band at 1705 cm^{-1} , the negative bands at 1680 and 1665 cm^{-1} , and a further decrease of the $1648(-)/1635(+)\text{ cm}^{-1}$ feature.

Previous studies of excitation transfer and trapping in RC-LH1 complexes have established that transfer of energy to the RC

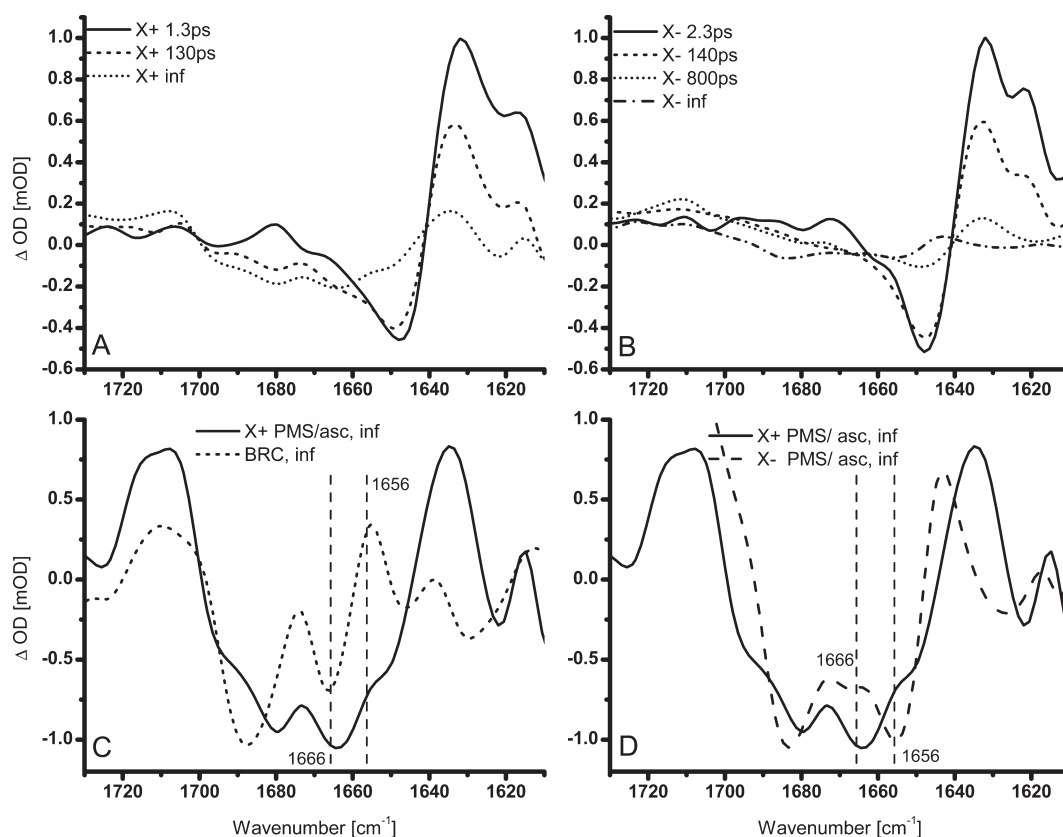


Figure 4. EADS for RC-LH1 complexes in ascorbate/PMS. (A) EADS obtained for RC-LH1-X+ complexes using a global analysis with increasing lifetimes of 1.3 ps, 130 ps, and an infinite component. (B) EADS obtained for RC-LH1-X- complexes using a global analysis with increasing lifetimes of 2.3 ps, 140 ps and an infinite component. (C) Comparison of final EADS for RC and RC-LH1-X+ complexes with marker bands typical for a $P^+Q_A^-$ state at 1656 and 1666 cm^{-1} highlighted. (D) Comparison of EADS for RC-LH1-X+ and RC-LH1-X- complexes with marker band inversion at 1656 and 1666 cm^{-1} highlighted. Spectra in panels C and D were scaled to facilitate comparison.

occurs over 30–70 ps.^{57–61,66} As a result, over a 3 ns measuring window the final state formed in both RC-LH1 and RC complexes is expected to be mainly $P^+Q_A^-$, as this state is formed in ~ 200 ps in isolated RCs and does not decay on the nanosecond time-scale. A caveat is that the presence of the antenna could allow for a small amount of detrapping, or long-lived antenna excited states in any LH1 complexes that are detached from RCs, and so the final difference spectrum of RC-LH1 complexes might be a composite of spectra of $P^+Q_A^-$ and LH1*. Figure 4C compares the EADS with an infinite lifetime for RCs (dashed line) and RC-LH1-X+ complexes (solid line). As can be seen, the sequence 1666(-)/1655(+) cm^{-1} characteristic for Q_A/Q_A^- in the spectrum of the RC (see above) was also present in the final spectrum of the RC-LH1-X+ complex (highlighted by the vertical lines in Figure 4C). The 1655(+) cm^{-1} component was less pronounced in the case of the RC-LH1 complex, appearing as a shoulder rather than a full band; this was probably due to the presence of LH1* contributions in this spectrum, signaled by the strong positive band at 1635 cm^{-1} . This should be accompanied by a negative LH1* band 1649 cm^{-1} , which would overlap and partially cancel out a positive Q_A^- band at 1655 cm^{-1} .

Ultrafast Mid-IR Spectroscopy of RC-LH1-X- Complexes.

Time-resolved spectra for the RC-LH1-X- complex were also recorded (Figure 4B) to determine whether the EADS for this complex differ substantially from those of the RC-LH1-X+ complex. A set of four components were required to fit the data with

lifetimes of 2.3 ps, 140 ps, 800 ps, and an infinite component. The initial EADS (Figure 4B, solid) was very similar to that of the RC-LH1-X+ complex, with a main differential feature at 1648(-)/1632(+) cm^{-1} and a positive band at 1622 cm^{-1} . This decayed in 2.3 ps to a second EADS (Figure 4B, dashed) that was also very similar to the second EADS obtained for RC-LH1-X+ complexes, with a decrease in amplitude of the positive bands at 1632 and 1622 cm^{-1} . The second component decayed in 140 ps to a third component, the EADS of which (Figure 4B, dotted) had a much smaller differential signal at 1649(-)/1633(+) cm^{-1} of only $\sim 10\%$ of the initial amplitude, a pronounced positive band at 1711 cm^{-1} , and negative bands at 1679 and 1649 cm^{-1} , respectively. The EADS of the final state (Figure 4B, dash-dotted line) had a relatively low amplitude compared to its predecessors. Thus, although the first two components required to fit the data for the RC-LH1-X+ and RC-LH1-X- complexes were similar in terms of line shape and amplitude, being dominated by spectral features indicative of LH1*, the subsequent components showed differences between the two sets of data.

Comparison of the final EADS for the RC-LH1-X+ and RC-LH1-X- complexes revealed that the characteristics of Q_A/Q_A^- seen in the spectrum of the RC-LH1-X+ complex (Figure 4D, solid), namely the sequence 1664(-)/1655(+), was absent in the spectrum of the RC-LH1-X- complex (Figure 4D, dashed line). Instead, this had a positive band at 1665 cm^{-1} , a negative band at 1655 cm^{-1} and a positive band at 1643 cm^{-1} , a pattern characteristic of a H_A/H_A^- difference spectrum (see data on RCs, above).

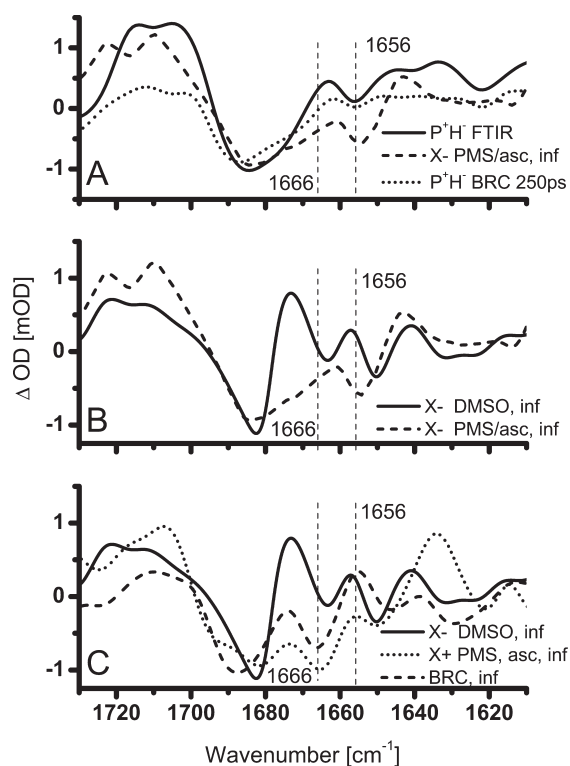


Figure 5. Influence of experimental conditions on the final readial pair formed in RC-LH1-X⁻ complexes. (A) Comparison of chemically generated FTIR spectrum of P⁺H⁻ in RCs with the final EADS for RC-LH1-X⁻ complexes in ascorbate/PMS and the RC EADS with a 250 ps lifetime attributed to P⁺H⁻ state. (B) Comparison of the final EADS for RC-LH1-X⁻ complexes in ascorbate/PMS and DMSO. Marker bands for P⁺H⁻ and P⁺Q_A⁻ at 1656 and 1666 cm⁻¹ are indicated. (C) Comparison of final EADS of RC-LH1-X⁺ and RC-LH1-X⁻ complexes in ascorbate/PMS and RC-LH1-X⁻ complexes in DMSO. Spectra were scaled to facilitate comparison.

This indicated that the final state achieved in the RC-LH1-X⁻ complex in the presence of mild reductant was P⁺H⁻ rather than the P⁺Q_A⁻ seen in the RC and RC-LH1-X⁺ complexes under the same conditions.

To test the reproducibility of this finding a second data set was recorded for both types of RC-LH1 complex under identical conditions. The final EADS obtained in two experiments carried out on RC-LH1-X⁺ and RC-LH1-X⁻ complexes are compared in Figure S3A and S3B, respectively, of the Supporting Information. The black spectra are from the data set also shown in Figure 4, the red spectra from the duplicate experiment. Despite some variation in baseline, the characteristic changes in sign of the final EADS around 1656 cm⁻¹ and 1666 cm⁻¹ were seen on comparing the data for the two types of RC-LH1 complex. For RC-LH1-X⁺ complexes (Figure S3A) the sequence 1666(-)/1655(+) cm⁻¹ characteristic for Q_A/Q_A⁻ (black spectrum) was also seen in the second data set (red spectrum) to within 2 cm⁻¹. In the second data set the positive band was more pronounced, peaking at 1657 cm⁻¹. For RC-LH1-X⁻ complexes (Figure S3B) the sequence 1665(+)/1655(-) cm⁻¹ characteristic for H_A/H_A⁻ (black spectrum) was reproduced as 1662(+)/1654(-) cm⁻¹ in the second data set (red spectrum). An averaged EADS was also calculated for both types of RC-LH1 complex (green).

To emphasize the finding that charge separation in RC-LH1-X⁻ complexes was blocked at P⁺H_A⁻, in Figure 5A the averaged

final EADS for the RC-LH1-X⁻ complex (dashed) is compared with the P_{H_A}/P⁺H_A⁻ difference spectrum from FTIR spectroscopy⁶⁷ (solid line) and the 250 ps (P⁺H_A⁻) EADS of the RC from the present work (dotted line). All three spectra have the distinct signature 1663(+)/1656(-)/1644(+) in common (within ±2 cm⁻¹), a signature quite distinct from the 1667(-)/1656(+)/1647(-) pattern expected for the state P⁺Q_A⁻.

Ultrafast Mid-IR Spectroscopy of RC-LH1-X⁻ Complexes under Oxidizing Conditions. Possible implications of charge separation being halted at the radical pair P⁺H_A⁻ in the RC-LH1-X⁻ complex are that Q_A is either already reduced, or is absent. To our knowledge, the properties of a PufX-deficient RC-LH1 complex have not been studied previously by ultrafast spectroscopy, but some study has been made of interactions between RC-LH1-X⁻ complexes and the cytochrome *bc*₁ complex through millisecond time-scale spectroscopy by Comayras and co-workers.^{68,69} In that study (and others) there was no indication that RC-LH1-X⁻ complexes assemble without a Q_A quinone. Rather, it was concluded that in membranes with PufX-deficient RC-LH1 complexes, reduction of the quinone pool leads to a larger degree of reduction of Q_A than is the case for membranes with RC-LH1-X⁺ complexes (70% Q_A⁻ with an 80% reduced pool vs 20% Q_A⁻ for RC-LH1-X⁺ complexes under the same conditions).^{68,69} The likely explanation of the data summarized in Figure 5A is therefore that under the experimental conditions charge separation in RC-LH1-X⁺ complexes produces (mainly) P⁺Q_A⁻ but in RC-LH1-X⁻ complexes produces (mainly) P⁺H_A⁻ because of the presence of Q_A⁻. This is in agreement with a low yield of P⁺H_A⁻ on the long time scale in the RC-LH1-X⁻ complexes, as in the presence of Q_A⁻ the state P⁺H_A⁻ recombines with a lifetime of several nanoseconds in isolated RCs.^{70,71}

The current observations add weight to an explanation put forward by Comayras and co-workers to account for the fact that RC-LH1-X⁻ complexes cannot support photosynthetic growth of *Rba. sphaeroides* under illuminated/anaerobic conditions in standard growth media. Such conditions are expected to produce a reduced quinone pool that would lead to larger than normal reduction of Q_A and a loss of charge separation in RC-LH1-X⁻ complexes compared with native RC-LH1-X⁺ complexes (see Discussion, below). In support of this, it has been found that photosynthetic growth can be restored to PufX-deficient strains of *Rba. sphaeroides* by supplementing the medium with the oxidant DMSO⁷²⁻⁷⁴ the explanation being that DMSO drains electrons from the quinone pool, oxidizing Q_A and restoring charge separation and light-driven cyclic electron transfer. This observation raises the question of whether the final state observed in RC-LH1-X⁻ complexes would be different in buffer supplemented with DMSO rather than ascorbate/PMS.

To test this, energy transfer, trapping and charge separation were examined by ultrafast spectroscopy of RC-LH1-X⁻ complexes suspended in 20 mM HEPES/D₂O (pD 7.6)/0.04% β-DDM/20 mM DMSO. In this case, a set of three components were required to fit the data, with lifetimes of 1.7 ps, 270 ps, and >3 ns (infinite). Figure 6A compares the EADS for the first component for RC-LH1-X⁺ and RC-LH1-X⁻ complexes in ascorbate/PMS (solid and dotted lines, respectively) and RC-LH1-X⁻ complexes in DMSO (dashed line). The spectra of the RC-LH1-X⁻ and RC-LH1-X⁺ complexes in ascorbate/PMS resembled each other very well, especially in the 1650 to 1630 cm⁻¹ region, and the associated lifetimes were similar (1.3 ps vs 2.3 ps). The initial EADS of the RC-LH1-X⁻ complex in DMSO (lifetime 1.7 ps) had the same general line shape, but the

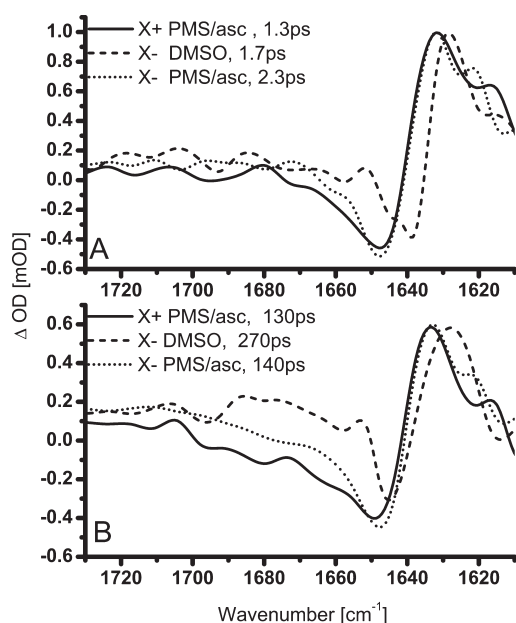


Figure 6. EADS for RC-LH1 complexes in ascorbate/PMS or DMSO. Comparison of the (A) first and (B) second EADS obtained using a global analysis with increasing lifetimes for RC-LH1-X⁺ and RC-LH1-X⁻ in PMS/ascorbate and RC-LH1-X⁻ complexes in DMSO.

dominant differential signal was shifted $\sim 11 \text{ cm}^{-1}$ toward lower wavenumbers. In addition the bleach around 1640 cm^{-1} was somewhat narrower than for the equivalent two spectra, with a shoulder at 1645 cm^{-1} .

Figure 6B compares EADS of the next component; again, correspondence between the spectra for the two complexes in ascorbate/PMS was high. The main variation for the second EADS of the RC-LH1-X⁻ complex in DMSO was qualitatively the same as that for the spectra of the initial component, with the main differential signal downshifted to lower wavenumbers and a narrowing of the ground state band at 1645 cm^{-1} . The associated lifetime of this component for RC-LH1-X⁻ complexes in DMSO was 270 ps, twice as long as the 130 and 140 ps seen for both types of complex in ascorbate/PMS, but closer to the 250 ps seen for the second component in isolated RCs in ascorbate/PMS and 222/280 ps for the same component in the absence of ascorbate/PMS.¹⁸

The final EADS of the RC-LH1-X⁻ complex in DMSO, and that from a duplicate experiment, are compared in Figure S3C (black and red, respectively). The pattern of positive and negative bands in the key region between 1640 cm^{-1} and 1680 cm^{-1} were similar in the two spectra, indicating good reproducibility in the character of the final state formed in the experiment, and an averaged spectrum was calculated (Figure S3C (green)). A comparison of this averaged EADS for the final component for RC-LH1-X⁻ complexes in DMSO and that for the same complex in ascorbate/PMS is presented in Figure 5B. Clear differences at $\sim 1666 \text{ cm}^{-1}$ and $\sim 1656 \text{ cm}^{-1}$ could be observed, with the signature $1662(+)/1655(-)$ in ascorbate/PMS changing to $1663(-)/1657(+)$ in DMSO, suggesting that addition of the oxidant had changed the final radical pair from $\text{P}^+\text{H}_\text{A}^-$ to $\text{P}^+\text{Q}_\text{A}^-$. To emphasize this, in Figure 5C, the final EADS for RCs in ascorbate/PMS (dashed), and averaged final EADS for RC-LH1-X⁺ complexes in ascorbate/PMS (dotted) and RC-LH1-X⁻ complexes in DMSO (solid) are overlaid. In all three

spectra, the $1666(-)/1656(+)$ cm^{-1} fingerprint of the $\text{P}^+\text{Q}_\text{A}^-$ radical pair was found (within an accuracy of $\pm 2 \text{ cm}^{-1}$), in marked contrast to the case of RC-LH1-X⁻ complexes in ascorbate/PMS where charge separation was limited to $\text{P}^+\text{H}_\text{A}^-$.

DISCUSSION

Investigating Charge Separation in RCs and RC-LH1 Complexes. The initial aim of the work described in this report was to investigate charge separation in *Rba. sphaeroides* RCs in the presence of the accompanying LH1 antenna protein. The kinetics and mechanism of this process have been studied extensively in purified RCs and in RCs in antenna-deficient membranes, but there have been only a very few studies of picosecond time-scale events in intact RC-LH1 complexes, and these have been limited to investigation of excitation trapping in membrane-bound complexes, employing *Rba. sphaeroides* mutants or other species that lack the peripheral LH2 antenna.^{57–61,75} To our knowledge, the present work is the first attempt to examine the dynamics of energy transfer and charge separation in a purified RC-LH1 complex.

One issue when studying energy transfer and excitation trapping in RC-LH1 complexes through near-IR pump/probe spectroscopy is that transient spectra are dominated by contributions from antenna excited states over a period of several hundred picoseconds.^{52–56} In addition, the absorbance difference spectra of the $\text{P}^+\text{H}_\text{A}^-$ and $\text{P}^+\text{Q}_\text{A}^-$ radical pairs in the near-infrared are somewhat similar, being dominated by bleaching of P ground state absorbance and a bandshift of the absorbance of the monomeric BChls at around 800 nm; differences between these spectra are confined to subtle changes in line shape in lower amplitude regions around 750–770 nm (e.g., see ref 76). By contrast, FTIR difference spectroscopy^{51,59–63} and more recent time-resolved mid-IR spectroscopy²⁰ have revealed characteristic signatures for $\text{H}_\text{A}/\text{H}_\text{A}^-$ and $\text{Q}_\text{A}/\text{Q}_\text{A}^-$ in the frequency range between 1640 and 1680 cm^{-1} , allowing the $\text{P}^+\text{H}_\text{A}^-$ and $\text{P}^+\text{Q}_\text{A}^-$ radical pairs to be distinguished. Accordingly, in the present study, charge separation in RC-LH1 complexes was investigated using ultrafast near-IR pump/mid-IR probe spectroscopy.

A second issue relevant to the study of energy transfer in RC-LH1 complexes is the requirement to utilize low excitation intensities in order to avoid quenching of the LH1 excited singlet state through singlet–singlet annihilation, as significant levels of such quenching could alter the kinetics of loss of the LH1* excited state on the time scale of a few picoseconds. Given the constraints of the experimental setup used for ultrafast spectroscopy in the present work, it was not possible to achieve experimental conditions that were guaranteed to be free of some singlet–singlet annihilation, and both the mid-IR measurements discussed below and the near-IR measurements discussed in the Supporting Information contained a fast 1.3–2.3 ps component that may have been contributed to by singlet–singlet annihilation. In addition, to our knowledge, the present work is the first to look at energy transfer and trapping in detergent-solubilized RC-LH1 complexes rather than complexes in intact membranes. Given these factors, the main focus of the present work was on the characteristics of the long-lived state achieved after photoexcitation of the two types of RC-LH1 complex studied, rather than on precise attribution of the earlier components that represent energy transfer and trapping.

A third issue when examining the properties of the RC-LH1 complex by laser spectroscopy is the problem of photogenerating a long-lived P^+ state that “closes” the RC. This issue is less

problematic in the case of purified RC because charge separation will lead to the formation of $P^+Q_A^-$ or $P^+Q_B^-$, which have lifetimes of 100 ms or 1 s, respectively ($P^+Q_A^-$ being formed in RCs where the Q_B quinone has been lost during purification). As a result, it is relatively straightforward to ensure that purified RCs are fully relaxed to the PQ_AQ_B ground state by combining a suitable rate of excitation pulses with movement of the sample and, perhaps, inhibition of Q_B^- formation. However, in more intact systems, there is the possibility of translocated electrons being lost to the ubiquinone pool, leaving a very long-lived P^+ state if the natural reductant (cyt c_2) is absent. To avoid this situation, previous studies of membrane-bound RC-LH1 complexes have employed the addition of sodium ascorbate and/or PMS to ensure slow reduction of P^+ between excitations.^{57–61,75} In the present study, RC-LH1 complexes were removed from the membrane and purified on sucrose density gradients, but it is known that such complexes are associated with a mini-pool of up to 15 ubiquinones, and the lifetime of the $P^+Q_B^-$ state is on the order of 3–5 times longer than in purified RCs.^{68,69,77,78} As a result, ultrafast mid-IR spectroscopy was carried out in the presence of sodium ascorbate and PMS to be consistent with previous work. These reagents have midpoint redox potentials (E_m) of around 40 mV and 50 mV, respectively, at pH 8.0,⁷⁹ which makes them suitable for reduction of P^+ ($E_m \sim 450$ – 500 mV, depending on the presence of membrane and antenna⁸⁰). However, they should not directly reduce Q_A , which has an E_m of -45 mV in isolated RCs⁸¹ and -80 mV in photosynthetic membranes at pH 8.0.⁸²

Characteristics of Energy- and Electron Transfer under Reducing Conditions. Ultrafast mid-IR spectroscopy was first applied to RCs, to determine whether the presence of sodium ascorbate and/or PMS would have a significant influence on the kinetics of primary or secondary charge separation, or on the lineshapes of the EADS attributed to the P^* , $P^+H_A^-$ and $P^+Q_A^-$ states formed. The EADS and associated lifetimes (4.1 ps, 250 ps and infinite) obtained for purified RCs in the presence of ascorbate/PMS (with 800 nm excitation) showed good correspondence to those determined in a previous study (3.6 ps, 280 ps, and infinite) obtained in the absence of ascorbate/PMS (with 860 nm excitation).¹⁸

Having established this, mid-IR spectroscopy was applied to RC-LH1 complexes in the presence of ascorbate and PMS. The dominant feature of the first and second EADS obtained for both types of RC-LH1 complex was a strong differential signal with a negative band corresponding to the ground state mode being at around 1648 cm^{-1} and a positive band corresponding to the downshifted excited state mode at around 1632 cm^{-1} . We attribute this feature to a downshift of the keto carbonyl modes of the LH1 antenna BChls on formation of the LH1* excited state. The equivalent strong downshift of the keto modes of the P BChls of the RC upon formation of P^* gave rise to a differential signal at $1688(-)/1668(+)\text{ cm}^{-1}$ (Figure 2, solid line). The size of the downshift was therefore similar in the two cases, 16 cm^{-1} and 20 cm^{-1} , respectively, but there was a strong difference ($\sim 40\text{ cm}^{-1}$) in the absolute positions of the two ground state modes in purified RCs and purified RC-LH1 complexes. It should also be noted that the peak frequency of this ground-state mode (1648 cm^{-1}) for the keto carbonyls of the LH1 BChls in the isolated RC-LH1-X+ and RC-LH1-X- complexes analyzed in the present study was somewhat lower than the 1661 cm^{-1} reported for the keto carbonyl groups of the LH1 BChls determined by FT-Raman spectroscopy of both RC-LH1-X+

and LH1-only complexes embedded in native *Rba. sphaeroides* membranes^{83,84} and purified *Rba. sphaeroides* LH1 complexes.⁸⁵

The reasons for low frequency of the ground-state mode of the LH1 keto carbonyls in the present study are not clear, but it is known that the stretching frequency of the keto carbonyl mode of chlorins and bacteriochlorins is sensitive to hydrogen bonding and the polarity of the surroundings of the group.⁸⁶ As an example, the stretching frequency of the keto carbonyl of BChl *a* has been reported to be at 1684 cm^{-1} in tetrahydrofuran but at 1652 cm^{-1} in hydrogen-bonding methanol,^{51,64} and this stretching frequency has been reported to be as low as 1635 cm^{-1} in BChl–water micelles.⁸⁷ The reason for the low stretching frequency observed for RC-LH1 complexes in the present report will require further investigation, but it is interesting to note that the position of this band further downshifted when ascorbate/PMS in the measuring buffer was replaced by 20 mM DMSO (Figure 6). This indicated that the stretching frequency was sensitive to the conditions of the experiment, one possibility being that these keto groups are engaged in hydrogen-bonds, and the strength of these was modulated by the conditions of the experiment (with a stronger hydrogen bond producing a lower frequency).

Although not yet explained, the strong difference in the line shape of the P/ P^* EADS in Figure 2 (solid line) and initial LH1/LH1* EADS in Figures 4A,B and 6 gave the possibility of assessing the contribution of the RC to the early spectral evolution of the system. In the case of both types of RC-LH1 complex, the 800 nm pump pulse achieved direct excitation of RCs as well as some excitation of the blue wing of the LH1 absorbance. On the basis of transient absorption in the near-IR, Xiao et al.⁶¹ concluded that excitation at 800 nm results in $\sim 50\%$ direct excitation of RCs, and that the probability of detraping of excitation energy to LH1 from P^* is very low, with a rate of 8 ps^{-1} . However, the contribution of RC* in $t = 0$ spectra for RC-LH1-X+ and RC-LH1-X- complexes (Figure 4A,B) was surprisingly small, and they appeared to be dominated by LH1* features. On the time scale of 1.3 and 2.3 ps, respectively, an RC $P^+H_A^-$ contribution became visible via the bleaching of the P-keto bands at 1688 cm^{-1} , representing primary charge separation between P and H_A , occurring via $P^* \rightarrow P^+B_A^- \rightarrow P^+H_A^-$, in the fraction of directly excited RCs. Note that also in the isolated RC this process is accompanied by an increase in the keto band around 1688 cm^{-1} . Concomitantly, a decay of LH1* signal takes place. As the current experiments were not performed under annihilation-free conditions, this process may represent singlet–singlet annihilation in LH1.

Attribution of the second component, with lifetimes of 130 and 140 ps, respectively, was less clear. In previous studies of energy transfer in membrane-bound RC-LH1 complexes from LH2-deficient strains of *Rba. sphaeroides* or *Rba. capsulatus*, a component of $\sim 46\text{ ps}$,⁵⁷ $\sim 37\text{ ps}$,⁶¹ or $\sim 72\text{ ps}$ ⁵³ has been reported, and interpreted as transfer of energy from the antenna to the RC (trapping), whereas slower minor components have been attributed to secondary electron transfer from $P^+H_L^- \rightarrow P^+Q_A^-$, or recombination of P^* from $P^+H_L^-$ in RCs where electron transfer to Q_A was blocked. In the present study, the lifetime of the second EADS could reflect these processes, perhaps originating from different sources given the evidence from the final EADS that the step $P^+H_L^- \rightarrow P^+Q_A^-$ was active in RC-LH1-X+ complexes but not in RC-LH1-X- complexes when ascorbate/PMS was present. In a parallel measurement employing near-IR pump/near-IR probe spectroscopy carried out on

RC-LH1-X⁻ complexes (see Supporting Information), a 43 ps component was obtained that was more consistent with what has been seen in previous work on membrane-embedded RC-LH1 complexes.^{52,53,56} We are currently investigating possible protocols for carrying out near-IR pump/mid-IR probe spectroscopy on membrane-embedded complexes, as well as carrying out more detailed side-by-side measurements of the two spectral regions, to better understand the basis of the 130/140 ps component seen in the mid-IR data.

One of the effects of DMSO was to alter the lifetime of this second EADS required to fit the time-resolved mid-IR spectra from 140 to 270 ps. A lifetime of 270 ps was close to the value of 250 ps obtained for the lifetime of P⁺H_A⁻ in RCs in ascorbate/PMS in the present study, and lifetimes of 280 and 222 ps obtained for RCs without oxidant or reductant in previous work.¹⁸ Again, precise attribution of this lifetime and explanation of why it varies will require further experiments and modeling.

Effect of PufX on the Final Charge Separated State in the RC-LH1 Complex. The most surprising finding in the analysis of the two types of RC-LH1 complex under mildly reducing conditions was the difference in the line shape of the final EADS, which had a lifetime in excess of the 3 ns time-window of the experiment. Again, bearing in mind the complex nature of the experiment with excitation of both antenna and RC at 800 nm, the line shape of the EADS obtained for the RC-LH1-X⁺ complex was consistent with that expected for P⁺Q_A⁻, with clear evidence of the spectral signature of the Q_A/Q_A⁻ transition. By contrast, the final EADS for the RC-LH1-X⁻ complex had a line shape consistent with P⁺H_A⁻, suggesting that Q_A was either absent from this complex or was (mainly) reduced under the particular experimental conditions. Replacement of mildly reducing ascorbate/PMS in the measuring buffer by mildly oxidizing DMSO (20 mM, E_{m,7.6} = 125 mV) led to a final EADS for the RC-LH1-X⁻ complex that now had the spectral signature of Q_A/Q_A⁻, showing that Q_A was not absent from this complex and that the contrasting results with ascorbate/PMS must have been due to Q_A being (mostly) oxidized in RC-LH1-X⁺ complexes and (mostly) reduced in RC-LH1-X⁻ complexes.

As outlined above, this finding provides support for a hypothesis put forward by Comayras et al. in 2005^{68,69} to explain the very strong effect of deletion of the gene encoding PufX on the capacity for growth of *Rba. sphaeroides* under standard anaerobic/illuminated heterotrophic conditions (see ref 30 for a detailed review). The RC-LH1 complexes that are assembled in these PufX-deficient strains have a higher-than-normal complement of LH1 BChls per RC (Figure 1b), and in *Rba. sphaeroides* it has been established that the LH1 antenna forms a closed cylinder of pigment-protein complex around the RC, rather than the open cylinder formed when PufX is present.^{37,38} Initially it was generally thought that this closed cylinder provides a physical obstruction to the exchange of ubiquinone/ubiquinol between the RC and cytochrome *bc*₁ complex. However, it was subsequently shown that PufX had minimal effects on such exchange under conditions where the quinone pool consisted of a mixture of ubiquinone and ubiquinol, but was important for ubiquinol release and/or diffusion to the *bc*₁ complex when the quinone pool was mostly oxidized, and ubiquinone diffusion and/or binding to the RC under conditions where the pool was mostly reduced.^{72,73} It was then established that there was a 2–3-fold slowing of the rate of turnover of quinone at the Q_B site of RC-LH1 complexes in the absence of PufX in both membranes and isolated complexes, and the rate of diffusion of quinol from the

RC to the cytochrome *bc*₁ complex was also slowed by a factor of 2.^{68,69} In addition, Comayras and co-workers showed that the rate of P⁺Q_B⁻ recombination was slowed by a factor of 4 in RC-LH1-X⁻ complexes, and the rate of the second electron transfer from Q_A to Q_B (i.e., the reaction Q_A⁻Q_B⁻ + 2H⁺ → Q_AQ_BH₂) was slowed by a factor of 6, both of which would indicate a stabilization of Q_B⁻ in the absence of PufX.^{68,69} Given this, Comayras and co-workers proposed that the lack of photosynthetic growth seen in PufX-deficient strains is due to most RCs being in the Q_A⁻ state under anaerobic/illuminated growth conditions, the rationale being that when Q_B⁻ is stabilized, the equilibrium of the above reaction will favor the Q_A⁻Q_B⁻ state. As a result, as the quinone pools and then Q_B becomes reduced under anaerobic conditions, Q_A will be more easily reduced in RC-LH1-X⁻ complexes than in RC-LH1-X⁺ complexes.

An attractive feature of this hypothesis is that it explains the observation that growth of PufX-deficient strains under anaerobic, illuminated conditions can be restored by supplementing the growth medium with DMSO.^{72–74} Here the rationale is that electron flow to DMSO partially oxidizes the ubiquinone pool, oxidizing Q_B and Q_A and opening the RC for catalysis of cyclic electron transfer despite the absence of PufX. In fact, it is known that anaerobic/illuminated growth of the closely related *Rba. capsulatus* on a strongly reducing carbon source such as butyrate or propionate is only possible if the medium is supplemented with an auxiliary oxidant such as DMSO in order to prevent over-reduction of the quinone pool and Q_A,⁸⁸ and redox poisoning of the *Rba. capsulatus* photosynthetic electron transfer chain by DMSO has been demonstrated experimentally.⁸⁹

The findings from ultrafast mid-infrared spectroscopy in the present work strongly support the hypothesis of Comayras and co-workers that a consequence of deletion of PufX is a deleterious shift in the redox equilibrium between Q_A, Q_B and the ubiquinone pool. The marked difference in the final radical pair state achieved in RC-LH1-X⁺ and RC-LH1-X⁻ complexes in the presence of ascorbate/PMS points toward Q_A being reduced in the latter but not in the former, despite the identical conditions used for bacterial growth, protein purification, and measurement of charge separation. It is not clear whether this difference in the redox state of Q_A was already present during cell growth, harvesting, and extraction/purification of RC-LH1 complexes, or whether it was induced by the use of ascorbate and PMS in the measuring buffer. However, it is clear that Q_A is (mostly) oxidized when charge separation is measured in RC-LH1-X⁻ complexes in the presence of DMSO, further validating the proposals of Comayras and co-workers^{68,69} and providing a neat correlation between results of ultrafast spectroscopy and measurements of the impact of DMSO on photosynthetic growth of PufX-deficient strains.^{72–74} What has emerged is a specific role for PufX in regulating the redox properties of Q_B to ensure that membrane-spanning charge separation to Q_A can still take place under conditions where the intramembrane quinone pool is mainly reduced. How PufX achieves this is as yet unclear, and further experiments are being directed toward understanding this.

CONCLUSIONS

Time-resolved mid-IR absorption difference experiments were performed on RC-LH1 complexes with and without the PufX protein. Our experiments show that PufX is required for

generation of the state $P^+Q_A^-$ in isolated complexes, as in the absence of PufX, electron transfer is blocked after the bacteriopheophytin acceptor. Experiments utilizing the oxidant DMSO showed that this blockage of membrane-spanning electron transfer was due to the presence of Q_A^- in PufX-deficient complexes under mildly reducing conditions rather than to the absence of Q_A . The data provide strong support for the hypothesis that one function of PufX is to ensure oxidation of Q_A^- under conditions of a reduced ubiquinone pool by preventing stabilization of Q_B^- by the LH1 antenna.

■ ASSOCIATED CONTENT

S Supporting Information. Near-IR pump–probe measurements on RC-LH1-X complexes, and details of reproducibility and averaging. This information is available free of charge via the Internet at <http://pubs.acs.org>.

■ ACKNOWLEDGMENT

L.I.C. and M.R.J. acknowledge funding from the Biotechnology and Biological Sciences Research Council of the United Kingdom.

Funding

This work is part of Research Programme ALW816.02.008, which is financed by the Netherlands Organisation for Scientific Research (NWO).

■ LIST OF ABBREVIATIONS

RC-LH1: reaction center-light harvesting complex 1
 DMSO: dimethylsulfoxide
 RC: reaction center
Rba: *Rhodobacter*
 BChl: bacteriochlorophyll
 Cyt: cytochrome c_2
 PMS: phenazine methosulphate
 P: primary electron donor
 H_A: bacteriopheophytin
 Q_A: ubiquinone

■ REFERENCES

- Allen, J. P.; Feher, G.; Yeates, T. O.; Komiyama, H.; Rees, D. C. *Proc. Natl. Acad. Sci. U.S.A.* **1987**, *84*, 5730.
- Chang, C. H.; Elkabbani, O.; Tiede, D.; Norris, J.; Schiffer, M. *Biochemistry* **1991**, *30*, 5352.
- Ermiler, U.; Fritzsche, G.; Buchanan, S. K.; Michel, H. *Structure* **1994**, *2*, 925.
- Jones, M. R. *Biochem. Soc. Trans.* **2009**, *37*, 400–407.
- Parson, W. W. In *Chlorophylls*; Scheer, H., Ed.; CRC Press: Boca Raton, FL, 1991; p 1153.
- Parson, W. W. In *Protein Electron Transfer*; Bendall, D. S., Ed.; BIOS Scientific Publishers: Oxford, 1996; p 125.
- Woodbury, N. W. In *Anoxygenic Photosynthetic Bacteria*; Blankenship, R. E., Madigan, M. T., Bauer, C. E., Eds.; Kluwer Academic Publishers: Dordrecht, The Netherlands, 1995; pp 527.
- Zinth, W.; Wachtveitl, J. *ChemPhysChem* **2005**, *6*, 871.
- Hoff, A. J.; Deisenhofer, J. *Phys. Rep.: Rev. Sect. Phys. Lett.* **1997**, *287*, 2.
- Okamura, M. Y.; Paddock, M. L.; Graige, M. S.; Feher, G. *Biochim. Biophys. Acta: Bioenerg.* **2000**, *1458*, 148.
- Wraight, C. A. *Front. Biosci.* **2004**, *9*, 309.
- Axelrod, H. L.; Okamura, M. Y. *Photosyn. Res.* **2005**, *85*.
- Hamm, P.; Zinth, W. *J. Phys. Chem.* **1995**, *99*, 13537.
- Hamm, P.; Zurek, M.; Mantele, W.; Meyer, M.; Scheer, H.; Zinth, W. *Proc. Natl. Acad. Sci. U.S.A.* **1995**, *92*, 1826.
- Haran, G.; Wynne, K.; Moser, C. C.; Dutton, P. L.; Hochstrasser, R. M. *J. Phys. Chem.* **1996**, *100*, 5562.
- Maiti, S.; Cowen, B. R.; Diller, R.; Iannone, M.; Moser, C. C.; Dutton, P. L.; Hochstrasser, R. M. *Proc. Natl. Acad. Sci. U.S.A.* **1993**, *90*, 5247.
- Maiti, S.; Walker, G. C.; Cowen, B. R.; Pippenger, R.; Moser, C. C.; Dutton, P. L.; Hochstrasser, R. M. *Proc. Natl. Acad. Sci. U.S.A.* **1994**, *91*, 10360.
- Pawlowicz, N. P.; van Grondelle, R.; van Stokkum, I. H. M.; Breton, J.; Jones, M. R.; Groot, M. L. *Biophys. J.* **2008**, *95*, 4089.
- Walker, G. C.; Maiti, S.; Cowen, B. R.; Moser, C. C.; Dutton, P. L.; Hochstrasser, R. M. *J. Phys. Chem.* **1994**, *98*, 5778.
- Wynne, K.; Haran, G.; Reid, G. D.; Moser, C. C.; Dutton, P. L.; Hochstrasser, R. M. *J. Phys. Chem.* **1996**, *100*, 5140.
- Remy, A.; Gerwert, K. *Nat. Struct. Biol.* **2003**, *10*, 637.
- Cogdell, R. J.; Gall, A.; Kohler, J. Q. *Rev. Biophys.* **2006**, *39*, 227.
- Cogdell, R. J.; Gardiner, A. T.; Roszak, A. W.; Law, C. J.; Southall, J.; Isaacs, N. W. *Photosyn. Res.* **2004**, *81*, 207.
- Hu, X. C.; Ritz, T.; Damjanovic, A.; Autenrieth, F.; Schulten, K. *Q. Rev. Biophys.* **2002**, *35*, 1.
- Roszak, A. W.; Howard, T. D.; Southall, J.; Gardiner, A. T.; Law, C. J.; Isaacs, N. W.; Cogdell, R. J. *Science* **2003**, *302*, 1969.
- Scheuring, S.; Levy, D.; Rigaud, J. L. *Biochim. Biophys. Acta: Biomembr.* **2005**, *1712*, 109.
- Scheuring, S. *Curr. Opin. Chem. Biol.* **2006**, *10*, 387.
- Sturgis, J. N.; Niederman, R. A. *Photosyn. Res.* **2008**, *95*, 269.
- Sturgis, J. N.; Tucker, J. D.; Olsen, J. D.; Hunter, C. N.; Niederman, R. A. *Biochemistry* **2009**, *48*, 3679.
- Holden-Dye, K.; Crouch, L. I.; Jones, M. R. *Biochim. Biophys. Acta* **2008**, *1777*, 613.
- Bahatyrova, S.; Frese, R. N.; Siebert, C. A.; Olsen, J. D.; van der Werf, K. O.; van Grondelle, R.; Niederman, R. A.; Bullough, P. A.; Otto, C.; Hunter, C. N. *Nature* **2004**, *430*, 1058.
- Francia, F.; Wang, J.; Venturoli, G.; Melandri, B. A.; Barz, W. P.; Oesterhelt, D. *Biochem.* **1999**, *38*, 6834.
- Jungas, C.; Ranck, J. L.; Rigaud, J. L.; Joliot, P.; Vermeglio, A. *EMBO J.* **1999**, *18*, 534.
- Qian, P.; Bullough, P. A.; Hunter, C. N. *J. Biol. Chem.* **2008**, *283*, 14002.
- Qian, P.; Hunter, C. N.; Bullough, P. A. *J. Mol. Biol.* **2005**, *349*, 948.
- Scheuring, S.; Francia, F.; Busselez, J.; Melandri, B. A.; Rigaud, J. L.; Levy, D. *J. Biol. Chem.* **2004**, *279*, 3620.
- Siebert, C. A.; Qian, P.; Fotiadis, D.; Engel, A.; Hunter, C. N.; Bullough, P. A. *EMBO J.* **2004**, *23*, 690.
- Walz, T.; Jamieson, S. J.; Bowers, C. M.; Bullough, P. A.; Hunter, C. N. *J. Mol. Biol.* **1998**, *282*, 833.
- Di Donato, M.; Cohen, R. O.; Diner, B. A.; Breton, J.; van Grondelle, R.; Groot, M. L. *Biophys. J.* **2008**, *94*, 4783.
- Pawlowicz, N. P.; Groot, M. L.; van Stokkum, I. H. M.; Breton, J.; van Grondelle, R. *Biophys. J.* **2007**, *93*, 2732.
- Di Donato, M.; Stahl, A. D.; van Stokkum, I. H. M.; van Grondelle, R.; Groot, M. L. *Biochemistry* **2011**, *50*, 480.
- Hunter, C. N.; Turner, G. J. *Gen. Microbiol.* **1988**, *134*, 1471.
- Jones, M. R.; Fowler, G. J. S.; Gibson, L. C. D.; Grief, G. G.; Olsen, J. D.; Crielaard, W.; Hunter, C. N. *Mol. Microbiol.* **1992**, *6*, 1173.
- Jones, M. R.; Visschers, R. W.; Van Grondelle, R.; Hunter, C. N. *Biochemistry* **1992**, *31*, 4458.
- McAuley-Hecht, K. E.; Fyfe, P. K.; Ridge, J. P.; Prince, S. M.; Hunter, C. N.; Isaacs, N. W.; Cogdell, R. J.; Jones, M. R. *Biochemistry* **1998**, *37*, 4740.
- McGlynn, P.; Hunter, C. N.; Jones, M. R. *FEBS Lett.* **1994**, *349*, 349.
- Crouch, L. I.; Holden-Dye, K.; Jones, M. R. *Biochim. Biophys. Acta, Bioenerg.* **2010**, *1797*, 1812.
- Groot, M. L.; van Wilderen, L.; Di Donato, M. *Photochem. Photobiol. Sciences* **2007**, *6*, 501.

- (49) van Stokkum, I. H. M.; Larsen, D. S.; van Grondelle, R. *Biochim. Biophys. Acta, Bioenerg.* **2004**, *1657*, 82.
- (50) Thibodeau, D. L.; Nabedryk, E.; Hienerwadel, R.; Lenz, F.; Mantele, W.; Breton, J. *Biochim. Biophys. Acta* **1990**, *1020*, 253.
- (51) Mantele, W.; Wollenweber, A.; Rashwan, F.; Heinze, J.; Nabedryk, E.; Berger, G.; Breton, J. *Photochem. Photobiol.* **1988**, *47*, 451.
- (52) Nabedryk, E. In *Infrared Spectroscopy of Biomolecules*; Chapman, H. H. M. a. D., Ed.; Wiley-Liss: New York, 1996; pp 39.
- (53) Nabedryk, E.; Andrianambintsoa, S.; Dejonghe, D.; Breton, J. *Chem. Phys.* **1995**, *194*, 371.
- (54) Nabedryk, E.; Bagley, K. A.; Thibodeau, D. L.; Bauscher, M.; Mantele, W.; Breton, J. *FEBS Lett.* **1990**, *266*, 59.
- (55) Brudler, R.; Degroot, H. J. M.; Vanliemt, W. B. S.; Steggerda, W. F.; Esmeijer, R.; Gast, P.; Hoff, A. J.; Lugtenburg, J.; Gerwert, K. *EMBO J.* **1994**, *13*, 5523.
- (56) Egorova-Zachernyuk, T. A.; Remy, A.; Shkuropatov, A. Y.; Gast, P.; Hoff, A. J.; Gerwert, K.; de Groot, H. J. M. *Vib. Spectrosc.* **1999**, *19*, 347.
- (57) Beekman, L. M.; van Mourik, F.; Jones, M. R.; Visser, H. M.; Hunter, C. N.; van Grondelle, R. *Biochemistry* **1994**, *33*, 3143.
- (58) Freiberg, A.; Allen, J. P.; Williams, J. C.; Woodbury, N. W. *Photosyn. Res.* **1996**, *48*, 309.
- (59) Timpmann, K.; Freiberg, A.; Sundstrom, V. *Chem. Phys.* **1995**, *194*, 275.
- (60) Timpmann, K.; Zhang, F. G.; Freiberg, A.; Sundstrom, V. *Biochim. Biophys. Acta* **1993**, *1183*, 185.
- (61) Xiao, W. H.; Lin, S.; Taguchi, A. K. W.; Woodbury, N. W. *Biochemistry* **1994**, *33*, 8313.
- (62) Bagley, K. A. In *Current Research in Photosynthesis*; Baltscheffsky, M., Ed.; Kluwer Academic Publishers: Dordrecht, The Netherlands, 1990; Vol. 1; p I.1.77.
- (63) Breton, J.; Thibodeau, D. L.; Berthomieu, C.; Mantele, W.; Vermeglio, A.; Nabedryk, E. *FEBS Lett.* **1991**, *278*, 257.
- (64) Mantele, W. G.; Wollenweber, A. M.; Nabedryk, E.; Breton, J. *Proc. Natl. Acad. Sci. U.S.A.* **1988**, *85*, 8468.
- (65) Breton, J.; Nabedryk, E. *Biochim. Biophys. Acta, Bioenerg.* **1996**, *1275*, 84.
- (66) Kennis, J. T. M.; Aartsma, T. J.; Ames, J. *Biochim. Biophys. Acta, Bioenerg.* **1994**, *1188*, 278.
- (67) Breton, J. In *Spectroscopy of Biological Molecules: Modern Trends*; Carmona, P., Ed.; Kluwer: Dordrecht, The Netherlands, 1997.
- (68) Comayras, F.; Jungas, C.; Lavergne, J. J. *Biol. Chem.* **2005**, *280*, 11203.
- (69) Comayras, F.; Jungas, C.; Lavergne, J. J. *Biol. Chem.* **2005**, *280*, 11214.
- (70) Gibasiewicz, K.; Pajzderska, M.; Ziolk, M.; Karolczak, J.; Dobek, A. J. *Phys. Chem. B* **2009**, *113*, 11023.
- (71) Tang, C.-K.; Williams, J. C.; Taguchi, A. K. W.; Allen, J. P.; Woodbury, N. W. *Biochemistry* **1999**, *38*, 8794.
- (72) Barz, W. P.; Francia, F.; Venturoli, G.; Melandri, B. A.; Vermeglio, A.; Oesterheld, D. *Biochemistry* **1995**, *34*, 15235.
- (73) Barz, W. P.; Vermeglio, A.; Francia, F.; Venturoli, G.; Melandri, B. A.; Oesterheld, D. *Biochemistry* **1995**, *34*, 15248.
- (74) Vermeglio, A.; Joliot, P. *Biochim. Biophys. Acta, Bioenerg.* **2002**, *1555*, 60.
- (75) Freiberg, A.; Timpmann, K.; Lin, S.; Woodbury, N. W. *J. Phys. Chem. B* **1998**, *102*, 10974.
- (76) van Brederode, M. E.; van Mourik, F.; van Stokkum, I. H. M.; Jones, M. R.; van Grondelle, R. *Proc. Natl. Acad. Sci. U.S.A.* **1999**, *96*, 2054.
- (77) Dezi, M.; Francia, F.; Mallardi, A.; Colafemmina, G.; Palazzo, G.; Venturoli, G. *Biochim. Biophys. Acta, Bioenerg.* **2007**, *1767*, 1041.
- (78) Francia, F.; Dezi, M.; Busselez, J.; Levy, D.; Rebecchi, A.; Mallardi, A.; Palazzo, G.; Melandri, B. A.; Venturoli, G. *Biochim. Biophys. Acta, Bioenerg.* **2004**, *1658*, 251.
- (79) Prince, R. C.; Linkletter, S. J. G.; Dutton, P. L. *Biochim. Biophys. Acta, Bioenerg.* **1981**, *635*, 132.
- (80) Visschers, R. W.; Vulto, S. I. E.; Jones, M. R.; van Grondelle, R.; Kraayenhof, R. *Photosyn. Res.* **1999**, *59*, 95.
- (81) Dutton, P. L.; Leigh, J. S.; Wraight, C. A. *FEBS Lett.* **1973**, *36*, 169.
- (82) Buchanan, S. K.; Dismukes, G. C.; Prince, R. C. *FEBS Lett.* **1988**, *229*, 16.
- (83) Olsen, J. D.; Sockalingum, G. D.; Robert, B.; Hunter, C. N. *Proc. Natl. Acad. Sci. U.S.A.* **1994**, *91*, 7124.
- (84) Olsen, J. D.; Sturgis, J. N.; Westerhuis, W. H. J.; Fowler, G. J. S.; Hunter, C. N.; Robert, B. *Biochemistry* **1997**, *36*, 12625.
- (85) Uyeda, G.; Williams, J. C.; Roman, M.; Mattioli, T. A.; Allen, J. P. *Biochemistry* **2010**, *49*, 1146.
- (86) Closs, G. L.; Katz, J. J.; Pennington, F. C.; Thomas, M. R.; Strain, H. H. *J. Am. Chem. Soc.* **1963**, *85*, 3809.
- (87) Ballschmiter, K.; Katz, J. J. *J. Am. Chem. Soc.* **1969**, *91*, 2661.
- (88) Richardson, D. J.; King, G. F.; Kelly, D. J.; McEwan, A. G.; Ferguson, S. J.; Jackson, J. B. *Arch. Microbiol.* **1988**, *150*, 131.
- (89) Jones, M. R.; Richardson, D. J.; McEwan, A. G.; Ferguson, S. J.; Jackson, J. B. *Biochim. Biophys. Acta* **1990**, *1017*, 209.
- (90) Potter, J. A.; Fyfe, P. K.; Frolov, D.; Wakeham, M. C.; van Grondelle, R.; Robert, B.; Jones, M. R. *J. Biol. Chem.* **2005**, *280*, 27155.